

1
2
3
4
5
6
7
8
9
10
11
12
13
14
15
16
17
18
19
20
21
22
23
24
25
26
27
28
29
30
31
32
33

SUPPLEMENTARY MATERIAL

1.0 Experimental cross-contamination: supplementary methods and results

1.1 Rotifer clones

To test the effect of adding two different animals to one tube, we selected two bdelloid rotifer clones from our cultures. One is the clone that provided DNA for the reference genome of *A. vaga* (Flot et al. 2013), which was kindly provided by K. Van Doninck in 2013. We believe it was collected originally in Italy (Mark Welch & Meselson 1998). We designate this clone "*A. vaga* (AD008)" or "*A. vaga* (genome)". The second clone was isolated from *Brachythecium rutabulum* (Hedwig), growing on *Quercus* sp. at Silwood Park, Ascot, UK (51° 24' 32.06" N 0° 38' 41.71" W), kept in continuous culture since 2012-01-09. We call this clone "*A. sp.* (AD006)". According to Debortoli et al. (2016), interspecific recombination occurred most often between the "cryptic species" A and E, and between C and E. These pairs of species share 86.1% and 86.4% sequence identity respectively at the mtCO1 marker. The identity between AD008 and AD006 at the mtCO1 marker is 86.5%, and thus commensurate with the species pairs involved in potential cross-contamination. Both clones were cultured using methods described previously (Wilson & Sherman 2010). Every two to three weeks, bdelloid populations were moved to fresh dishes of sterile distilled water over Czapek-Dox 0% agar (Barron 2004). Cultures were fed with a standardised inoculum of *Escherichia coli* (OP50), and *Saccharomyces cerevisiae* (S288c).

1.2 Design and replication

We prepared 12 tubes, divided into three groups and replicated as shown in Table S1. Biological replicates refer to different tubes, technical replicates refer to repeated PCR and sequencing using the same tube of template DNA. For each of the groups (1X6, 1X8, 2X6-8), one biological replicate was selected for technical triplication. For the 2X6-8 group, a further two biological replicates were selected for technical duplication.

1.3 Rotifer isolation

34 For our experiment, it was critical to be certain of the exact number of rotifers in each tube. The
35 methods and citations provided by Debortoli et al. (2016) do not describe the technique used to
36 isolate animals. We requested a protocol from the authors, and were given the following summary:

37

38 "Our procedure is simple, we collect the lichen/grass patch and put it in Spa® water overnight. The
39 next day, we isolate the individuals identified as *A. vaga* by pipetting and washing them in clean
40 water drops (serial dilutions). We then carefully checked under the binocular each tube to make sure
41 that only one individual was present." (N. Debortoli and K. Van Doninck, pers. comm.)

42

43 This description raised some technical concerns for us. Prior to 2014, we had employed a similar
44 procedure, but we found that pipettes were unsuitable for systematic isolation of individuals from
45 nature, and that quality control procedures requiring visual inspection of Eppendorf tubes were
46 inherently unreliable. Bdelloid rotifers are tiny, transparent and often rest motionless and invisible
47 under the distortion of a meniscus or against the plastic base of a tube. They frequently stick inside
48 pipette tips and are very difficult to dislodge or even to see. This leads to lost time and plasticware,
49 and more seriously, to loss of specimens and bias in the subset of animals that successfully pass
50 through the protocol. We occasionally experienced contamination via the following events. An
51 individual is serially washed and deposited into a tube by pipette. The tube is carefully checked
52 under the binocular microscope, but no animal is detected. It is assumed that the specimen was
53 stuck in the pipette tip, but this cannot be directly verified. The tip is changed, and a second rotifer
54 is serially washed and placed in the tube. This time, when the tube is carefully checked, a rotifer is
55 visually confirmed, and the tube is sealed for DNA extraction. In fact, the first animal also entered
56 the tube, but was hidden under the meniscus or on the bottom; thus, two rotifers now share one
57 tube. This is not a particular problem when isolating animals from a clonal culture, but becomes a
58 critical technical issue when isolating genetically different animals from nature. Opportunities for
59 contamination increase when large numbers of animals must be isolated.

60

61 To address these problems, we now use a needle-based protocol when isolating individuals. This
62 protocol is described in Additional File 1, and was used to prepare experimentally cross-
63 contaminated samples. Into each of the 12 experimental tubes, 8µL of sterile Milli-Q water was
64 pipetted. To each tube in groups 1X6 and 2X6-8, the needle protocol was used to move a single
65 rotifer from a stock culture of *A. sp.* (AD006), via a wash droplet of 1mL sterile Milli-Q water. To
66 each tube in groups 1X8 and 2X6-8, a single rotifer was moved from a stock culture belonging to *A.*
67 *vaga* (AD008). The tubes in group 2X6-8 therefore contained two rotifers, one from each species.

68

69 **1.4 DNA extraction and sequencing**

70

71 We extracted DNA from the samples and amplified the mitochondrial cytochrome oxidase I (mtCO1)
72 marker by PCR using the methods described by Debortoli et al. (2016). We used the same primers
73 (LCO1 and HCO1; Folmer et al. 1994) at the same concentrations, and the same concentration of
74 template in the same reaction volume (25µL). Amplifications were performed using GE Healthcare
75 illustra™ PuReTaq Ready-To-Go PCR Beads. PCR products were purified, and sequenced in both
76 directions with the same primers using an ABI 3730xl DNA Analyzer (Applied Biosystems), via a
77 commercial Sanger sequencing service (Macrogen Europe, Amsterdam, The Netherlands).

78

79 **1.5 Replicability of results**

80

81 Technical replicates within the 2X6-8 group were concordant and the same clone always dominated
82 the amplicon pool, but biological replicates showed different dominant clones (Table S2). For three
83 samples, *A. vaga* (AD008) supplied the majority haplotype (99.5%, 99.3% and 99.6% of bases called);
84 for the other three samples, *A. sp.* (AD006) was in the majority (99.6%, 99.7%, 97.9%). Concordance
85 among technical replicates suggests that small differences in efficiency of lysis or DNA extraction are
86 at least as important as differences during PCR in determining which of the genomes is amplified.
87 Consequently, it may not be surprising to see a consistent majority sequence when amplifying
88 repeatedly from the same sample, even if it contained multiple animals. The discordance among
89 biological replicates suggests that the direction of the bias may be inconsistent between samples,
90 even when the same two species are involved.

91

92 Figure 1 presented results from bidirectional pairs of sequencing chromatograms for Samples
93 1X6_01a and 2X6-8_03a, where *A. sp.* (AD006) was in the majority and *A. vaga* (AD008) in the
94 minority. To check robustness in the reciprocal case, we repeated the analysis for Samples 1X8_02c
95 and 2X6-8-05a, where *A. vaga* (AD008) was in the majority. The outcomes were as expected (Figure
96 S1). Again, the minority peaks for AD008 often were hidden within noise associated with
97 polymerase slippage and other errors, but the contaminant was recovered via ConTAMPR.

98

99 **2.0 Methods for chromatogram quality analysis**

100

101 Sequencing chromatograms for our experimental samples were returned by MacroGen Europe in the
102 ABIF format, which included phred quality scores (Ewing & Green 1998). Chromatogram files were
103 provided by Debortoli et al. in the .scf file format. We used CodonCode Aligner (v. 7.0.1, CodonCode
104 Corporation) to assign phred quality scores to these chromatograms, which were imported for
105 further processing in Geneious (v. 8.1.9, Biomatters Ltd, Auckland, New Zealand; Kearse et al. 2012).

106
107 Chromatograms for mtCO1 were uniformly trimmed to 605bp to avoid sequencing artefacts near the
108 priming sites, and phred Q20 quality scores are reported for this section. The boxplots shown in
109 Figures 4 and 5 were produced using R (v. 3.3.1, R Core Team) with the default setting for whisker
110 length, and annotated manually. The two distributions were plotted separately in Figure 4 because
111 they were statistically different. Owing to obvious outliers, distributions of quality scores for the
112 chromatograms of Debortoli et al. (2016) were not assumed to be normal, and were compared using
113 the Mann-Whitney test, implemented in R through the "wilcox.test" function. The equivalent
114 distributions for our new data were approximately normal, but the difference between groups was
115 not significant whether analysed using a parametric (N=38, t=1.13, P = 0.26) or nonparametric
116 approach (N=38, Mann-Whitney W=234, P=0.1186).

117
118 The 28S ribosomal marker was amplified by Debortoli et al. in four overlapping fragments. This locus
119 is highly conserved among even distantly related species. We restricted all our analyses to the first
120 fragment, amplified with the primers 28S0FCT and 28S1RCT (Debortoli et al. 2016). Among the six
121 *Adineta* species reported by Debortoli et al (2016), this fragment has 70 variable sites in 700bp
122 (10%), whereas only 24 variable sites are found in the remaining 1610bp (1.5%). We trimmed
123 chromatograms to a uniform length of 659bp (28S0FCT) or 666bp (28S1RCT) and calculated phred
124 quality scores for this informative region. We focused on the Q40 phred score because the overall
125 quality of 28S chromatograms was higher than for mtCO1; we suggest that the whole-genome
126 amplification step tended to increase the representation of a single template and reduced or
127 eliminated competing signals, especially after further PCR.

128
129 The distribution of 28S quality scores was shifted significantly lower for samples where HGT was
130 claimed (Figure 4, Mann-Whitney Test: N=122, W=373.5, P=0.015). Both the median and second-
131 highest quartile of the "HGT" samples fall within the second-lowest quartile of the "non-HGT"
132 samples. The HGT group also had significantly more files with scores below 80% (Fisher's Exact Test,
133 4 in 12 versus 2 in 121, P=0.0006; or if we treat paired chromatograms from the same sample as
134 non-independent, 2 in 6 versus 1 in 60, P=0.019).

135

136 No attempt was made to assess quality scores for EPIC25 chromatograms, because even if DNA all
137 comes from a single animal, these amplicons represent a pair of homologous intronic regions that
138 frequently are separated by at least one insertion-deletion polymorphism (indel), which means two
139 sets of peaks are superimposed out-of-phase in some regions (Debortoli et al. 2016), rendering
140 quality scores uninformative.

141

142 **3.0 Contingency table analysis of minority peak ranks (ConTAMPR)**

143

144 **3.1 Multiple sequence alignments**

145

146 The sequences of all haplotypes delimited by Debortoli et al. (2016) were retrieved from GenBank
147 (KU860573–KU861170), along with relevant sequences for the *A. vaga* reference clone (GQ398061;
148 JX184001), *A. ricciae* (EF173187; KM043216) and *A. sp.* AD006 (KM043183). Multiple alignment of
149 chromatograms and candidate sequences was performed using MAFFT v. 7.017 (Katoh et al. 2009),
150 implemented in Geneious using the MAFFT plugin (v. 1.3.3). For some sequences, particularly
151 mtCO1, this algorithm alone was sufficient to bring peaks for the majority and putative minority
152 sequences into alignment with the reference haplotypes. This is because there are no indels
153 between species for the mtCO1 marker, so peaks corresponding to amplicons from different
154 templates are superimposed ('in-phase'), though we typically saw slight displacement of minority
155 peaks by less than a base-width in one direction or another relative to the majority peak. This is
156 illustrated in Additional File 2, using annotated screenshots from the visual interface of Geneious.

157

158 For 28S rDNA, a multiple alignment of all unique sequences for *A. vaga* Species A-F revealed three
159 indels of 1-2bp within a single 100bp region of the focal first fragment (Figure S2). This occasionally
160 created challenges in testing whether two sequences from different species were present in an
161 amplicon population. For instance, Sample B14 was predicted to include haplotypes from Species A
162 and E. There is a single 1bp indel between these species (at position 134 in Figure S2), which means
163 the minority peaks in a forward chromatogram are predicted to run approximately in-phase with the
164 majority peaks until the indel, then become misaligned by 1bp, whereas the minority peaks in a
165 reverse chromatogram will show the opposite pattern. The contaminant might thus be mistaken for
166 a polymerase slippage artefact (Mullis et al. 1994). To analyse such a pattern, it is necessary to
167 manually shift the alignment of each chromatogram by 1bp around the indel, which means the
168 majority peaks are out of phase with the aligned majority haplotype for part of its length. This

169 alignment shift is illustrated in Additional File 3. For clarity, we point out every base corresponding
170 to the minority Species E haplotype in both directions. The pattern of multiple peaks changes
171 exactly as predicted at the site of the 1bp indel between Species A and Species E, which thus
172 represents further, sequence-independent evidence for the additional haplotype.

173

174 EPIC25 is a highly variable intronic marker with multiple indels of up to 12bp within and 23bp
175 between *A. vaga* Species A-F. Superimposed sequences from different species are therefore
176 displaced even further and more frequently than at 28S, which makes it challenging to align even
177 one candidate haplotype to the minority peaks. Multiple manual adjustments to an initial MAFFT
178 alignment were necessary to follow the minority haplotype after each indel. It would not be feasible
179 to attempt to align haplotypes from more than two candidate species at once against these
180 chromatograms, since the peaks and variable sites would almost never be predicted to coincide with
181 both candidates. However, it was not necessary to align every species individually to test for the
182 EPIC25 sequences listed in Table 1, because the predicted matches were so clear and the alignment
183 constraints made a match to any alternative haplotype so improbable. Additional File 4 illustrates
184 the alignment shifts necessary to follow a minority Species A haplotype running alongside a Species
185 E haplotype with at least 5 dispersed indels of varying lengths. Each peak we interpret as
186 corresponding to the minority haplotype is individually highlighted.

187

188 **3.2 Peak rank assignments**

189

190 After bidirectional pairs of chromatograms had been aligned with candidate sequences, we manually
191 scored the relative heights of minority fluorescence peaks at each site where a candidate sequence
192 differed from the majority haplotype. We examined the trace lines corresponding to the remaining
193 three nucleotides. Where these formed clear peaks, we assigned ranks 2, 3 and 4 based on their
194 relative heights, and recorded the rank corresponding to the required base for each candidate
195 sequence. The absolute heights were not considered, because we determined experimentally that
196 peaks corresponding to a known second animal may be very small, inconsistent or even absent
197 (Figure 1). Where two peaks appeared equal in height, we increased the magnification of the
198 chromatogram using the Geneious interface until a difference, however small, became clear. If no
199 such difference was apparent, the available ranks were randomly assigned to the two peaks.

200

201 When the minority sequence was 1bp out of phase with the majority haplotype, minority bases
202 sometimes did not correspond to distinct peaks, but produced either a trailing or a leading 'tail'

203 attached to the preceding or succeeding peak. In these cases, there was usually a local maximum or
204 at least an inflection point which we took as the height of the peak. If a base did not correspond to a
205 clear peak, local maximum or inflection point, we estimated the mean relative heights of the trace
206 lines at that site, regardless of shape. Where the trace line for a nucleotide showed absolutely no
207 signal at a site, we recorded rank "5" to indicate this feature, but treated it as a fourth-ranked peak
208 call for the purpose of analysis. Very rarely, the trace lines for two nucleotides both were flat, with
209 no fluorescence signal. In these cases, the two missing nucleotides were each annotated as "6", and
210 these were later split equally between ranks 3 and 4 for analysis.

211

212 At a locus like mtCO1, where all sequences are 'in-phase', the majority peak by definition cannot be
213 called to represent a minority variant. However, Additional Files 3 and 4 illustrate a complication
214 that occurs when majority and minority peaks are not aligned in phase, as at 28S and EPIC25.
215 Sometimes, the expected minority peak at a variable site will happen to match the out-of-phase
216 majority peak. This is a pure coincidence, but it prevents an assessment of how high the predicted
217 secondary peak would have been otherwise, and it is not trivial to predict how often this is expected
218 to happen under the null hypothesis. Where the "minority" haplotype happened to match a shifted
219 majority peak, we recorded "1" as the rank, and we took a conservative approach and simply
220 excluded all of these first-ranked "minority" calls from contingency analyses.

221

222 **3.3 Statistical analysis of contingency tables**

223

224 If minority peaks are a consequence of noise, non-rotifer contaminants, polymerase slippage or
225 other sequencing artefacts, then all else being equal we predicted that the peak ranks corresponding
226 to any control rotifer sequence would not differ significantly from an equal distribution (i.e. a 1:1:1
227 ratio for second, third and fourth-ranked peaks). We validated this prediction using chromatograms
228 from our "1X" experimental groups (e.g. Figure S1). Alternatively, if a second haplotype is present,
229 the set of peaks corresponding to that haplotype ought to differ significantly from the null
230 distribution, showing a significant bias in favor of second- rather than third-ranked peaks, and third-
231 rather than fourth-ranked peaks. For each candidate haplotype, we tested whether the peak rank
232 distribution differed significantly from the null hypothesis of a 1:1:1 ratio, using Pearson's Chi-
233 squared test for count data (Agresti 2007), implemented in R via the "chisq.test" function.

234

235 In many cases, more than one alternative sequence produced a significant deviation from the null
236 distribution. This is expected, because at many variable sites an alternative base is shared by more

237 than one rotifer species; therefore, the true matching sequence will also 'drag' the rank distribution
238 of species that share bases. For example, in Figure 1B, the *A. ricciae* control sequence deviates from
239 the null expectation ($\chi^2=64.9$, d.f. =2, $P = 8.07 \times 10^{-15}$), but only because it shares some variants with
240 *A. sp.* (AD006). Excluding these shared sites abolishes the apparent fit ($\chi^2= 3.2$, d.f. = 2, $P=0.202$).
241 The effect of relatedness is further illustrated in Figure 3. To distinguish the primary match, we
242 compared the degree of fit not only against the null distribution, but among different candidate
243 species. We typically used the Chi-square test of independence for a 3 x n contingency table, where
244 n is the number of candidate species or haplotypes. If the initial table included cell counts too small
245 to meet the assumptions of the test, two or more control species were pooled. Table 1 indicates the
246 species or haplotypes that were used for each comparison; distributions that were pooled are
247 indicated with "&". In some cases, further pairwise contrasts are reported in the text. To correct for
248 the problem of multiple comparisons, α was adjusted using the Bonferroni correction, but all
249 hypothesis tests remained significant even using this highly conservative approach.

250

251 **4.0 Neighbor-joining phylogeny**

252

253 The phylogenetic tree in Figure 3 was constructed using the neighbor-joining method implemented
254 in the Geneious Tree Builder tool, with the default settings and 100 bootstrap replicates.

255

256 **5.0 Supplementary results for samples with evidence of "interspecific DNA transfers"**

257

258 Analysis of chromatograms for the six apparently incongruent samples indicated that some
259 contained DNA from more than one animal, while others contained the predicted "original copies"
260 of genes that had supposedly been replaced via "interspecific horizontal genetic transfer". The
261 results are summarised in Table 1, and this section discusses each of the samples in greater detail.

262

263 **5.1 Sample B11**

264

265 To test the hypothesis of cross-contamination for Sample B11, it was necessary to predict which 28S
266 and mtCO1 haplotypes a putative second animal from Species E might have. We consulted Table S3
267 of Debortoli et al. (2016), and found that only Individual 81 [E] shares all the Species E haplotypes
268 that feature incongruently in Sample B11. We therefore aligned the B11 chromatograms to the
269 haplotypes of that individual: Hap31 [E] at mtCO1, and Hap13 [E] at 28S. The choice of control
270 haplotypes to represent each of the other species (Figure 2) was random. Peak rank distributions for

271 the six control species were statistically indistinguishable from each other ($\chi^2=6.66$, d.f. = 10, P =
272 0.76), and only differed from the null expectation because each happened to share some bases with
273 Hap31 [E]. For example, if we exclude polymorphisms *A. ricciae* shares with Hap31 [E], it no longer
274 differs from an equal ratio of second, third and fourth peaks (30:40:26; $\chi^2=3.25$, d.f. = 2, P = 0.197).

275

276 Although ConTAMPR revealed additional mtCO1 and 28S haplotypes for Sample B11 (Figure 2; Table
277 1; Additional File 2), the corresponding chromatograms are not obvious outliers in terms of phred
278 quality scores (Figure 4; Figure 5). At 28S, for instance, both chromatograms for Sample B11 lie
279 within the interquartile range for samples where no HGT is claimed. This is consistent with the
280 results of our experiments: even when multiple animals are present, we do not necessarily see
281 obvious differences in chromatogram quality, since minority peaks may be very small, or absent.

282

283 If Sample B11 contained two animals, it is interesting that the majority haplotypes for mtCO1 and
284 28S were from Species A, whereas those at EPIC25, EPIC63 and Nu1054 were from Species E. This
285 may simply reflect the chance outcome of two consecutive nonlinear amplifications (WGA and PCR).
286 However, the guanine-cytosine (GC) content of the Species A haplotypes expected at EPIC25, EPIC63
287 and Nu1054 is much higher than the corresponding Species E haplotypes that Debortoli et al.
288 recovered (+17.7%, +13.6%, +21.2% respectively), whereas GC differences were much lower at
289 mtCO1 and 28S (+1.9%). The whole-genome amplification kit used by Debortoli et al. has a known
290 bias in favor of templates with lower GC content (Han et al. 2012), and multi-template PCR also is
291 sensitive to this parameter (Polz & Cavanaugh 1998). Substantial differences in GC content may
292 have helped to skew amplification of the competing haplotypes, effectively masking Species A at
293 EPIC25, EPIC63 and Nu1054. At mtCO1 and 28S, GC was not substantially different, and the
294 identities of both animals were recovered via ConTAMPR, though their representation was far from
295 equal. Owing to effects like this, absence of evidence is not evidence of absence when considering
296 amplicons from potentially contaminated samples. Even if two animals are present, one may be
297 masked by the other at certain loci or in certain amplifications. It is very difficult to exclude the
298 hypothesis of contamination on the basis of apparently clean chromatograms, but it is immediately
299 telling to discover an extra haplotype.

300

301 **5.2 Sample B22**

302

303 The predicted donor of the incongruent EPIC25 haplotype in "Individual 58" was Species E. In
304 animals of this species, Table S3 of Debortoli et al. (2016) shows that EPIC25 Hap37 [E] occurs with

305 mtCO1 Hap29 [E] and 28S Hap16 [E]. For ConTAMPR, we therefore aligned the B22 mtCO1 and 28S
306 chromatograms against these candidates, along with control sequences from other species. Again,
307 we found evidence for the predicted haplotypes (Figure S3, Figure S4). The extra 28S haplotype in
308 Sample B22 was sufficiently prominent that the phred quality scores for these chromatograms fell
309 outside the range of values for samples where no HGT was claimed (Figure 4).

310

311 We examined chromatograms for Sample B22 at the EPIC25 marker itself, where the authors
312 reported a single, incongruent haplotype: Hap37 [E]. We did not find evidence for an expected
313 'native' Species C sequence. We suggest this haplotype was lost either during PCR or WGA, perhaps
314 in part because its GC content would have been approximately 22% higher than Hap37 [E].

315

316 The authors characterised "Individual 58" as "homozygous" at EPIC25. However, it is clear from the
317 data that a second Species E haplotype also was present in Sample B22. The trace files show
318 hundreds of double and triple peaks of comparable heights. As discussed above, these represent
319 two genomic homologs, running slightly out of phase following an indel, and with triple peaks
320 indicating further single nucleotide polymorphisms (SNPs) between them. There are at least 7 SNPs
321 between Hap37 [E] and the other haplotype in Sample B22, along with the indels. Many of these
322 appear to correspond to standing polymorphisms shared by other animals in the Species E
323 population (Figure S5). The presence of two rather divergent "transferred" haplotypes in a putative
324 "recipient individual" is important. It is not consistent with the HGT scenario posited by Debortoli et
325 al. (2016), in which "interspecific recombination" replaced the original DNA at one site, and "gene
326 conversion promptly copied the integrated DNA on its homologous region". That would produce
327 two identical haplotypes in the recipient. It would not preserve various SNPs and indels found in a
328 "heterozygous" donor. On the other hand, this pattern is predicted if the haplotypes arose from a
329 contaminating animal belonging to Species E, which had heterozygous combinations at EPIC25
330 similar to those seen in Individuals 81 (Hprim14a/b) and 78 (B39a/b). This is an independent line of
331 evidence for the conclusions supported by ConTAMPR at 28S and mtCO1.

332

333 **5.3 Sample B39**

334

335 Debortoli et al. (2016) interpreted Sample B39 as Individual 66 [E]. A Species E mtCO1 haplotype
336 had been replaced, in their view, by one imported from Species C. An alternative hypothesis is that
337 Sample B39 was cross-contaminated with some DNA from Species C, which happened to be
338 amplified by the mtCO1 primers instead of the native sequence. This hypothesis predicts a Species E

339 haplotype congruent with the other loci among the minority mtCO1 amplicons. Specifically, Table S3
340 of Debortoli et al. (2016) indicates that Individual 66 ought to have mtCO1 Hap31 [E], as seen in
341 Individual 81. Like Individual 66, that animal had Hap16 [E] at 28S, Hap16 [E] at EPIC63, Hap19 [E] at
342 Nu1054 and Hap30 [E] at EPIC25. No other individual had such a combination.

343

344 We used ConTAMPR to test whether minority peaks might correspond to Species E rather than any
345 other species, and also to Hap31 [E] rather than any other Species E mtCO1 haplotype. We aligned
346 B39 chromatograms not only to other *Adineta* species, but to seven diverse haplotypes from Species
347 E. We found strong and specific evidence for the 'missing' native mtCO1 haplotype predicted for
348 Individual 66 (Figure S6). This result brings all five loci into concordance without the need to invoke
349 "interspecific horizontal genetic transfer" or transformation of mtDNA, which is problematic in itself
350 (Larosa & Remacle 2013). The only incongruence in Sample B39 is the presence of mtCO1 Hap 10 [C]
351 among the amplicons. We attribute this either to chance amplification from loose Species C mtDNA
352 associated with the surface or gut of Individual 66, or to a second animal whose nuclear sequences
353 were dropped or outcompeted during WGA or PCR, as seen with samples B11 and B22.

354

355 **5.4 Samples B14 and B3B1**

356

357 For samples B14 and B3B1, the minority peaks in mtCO1 chromatograms were a significantly better
358 match to several other bdelloid mtCO1 haplotypes than the null expectation. This is consistent with
359 the presence of additional mtCO1 sequences, and therefore DNA from additional animals in these
360 samples (Figure S7). However, the peak rank distributions for several candidate species could not be
361 distinguished statistically when compared with each other.

362

363 Looking at other loci, we noticed that B14 and B3B1 were the only samples to show unambiguous
364 evidence of haplotypes originating from at least three different species (in each case, A, C and E;
365 Table 1). We guessed that we were unable to identify a single consistent secondary sequence at
366 mtCO1 because three animals from quite different species had contributed DNA to these samples.
367 This hypothesis was supported by the fact that mtCO1 chromatogram from these two samples were
368 extreme outliers in quality (Figure 5). The presence of DNA from three animals would explain why
369 additional mtCO1 haplotypes cannot be narrowed down to a single candidate. Relative to the subtle
370 minority peaks produced when we added just one extra animal (Figure 1B), the noise in these
371 chromatograms is such that almost any *Adineta* haplotype could be present. The hypothesis of

372 "interspecific horizontal genetic transfers" supplies no obvious explanation for the unusual features
373 of the mtCO1 amplicon population from these particular samples.

374

375 For Sample B14, we found evidence of an additional haplotype at 28S, consistent with Species E and
376 a better match by a significant margin than more distantly related species (Figure S8). This suggests
377 that one of the additional animals belonged to Species E, which would explain the incongruent
378 Species E haplotypes Debortoli et al. (2016) found at EPIC63 (Table 1). Peaks corresponding to this
379 additional haplotype also explain the unusually low phred quality scores for the 28S chromatograms
380 for Sample B14 (Figure 4). These peaks are annotated fully in Additional File 3. The absolute heights
381 of secondary peaks were often very low, as we saw at mtCO1 when we deliberately added two
382 animals. At 28S, this may reflect preferential nonlinear amplification of one haplotype during both
383 WGA and PCR. This would explain why some of the other contaminated samples (e.g. B11) did not
384 show obviously anomalous 28S quality scores, or sometimes any detectable second 28S haplotype
385 (e.g. B3B1). Conversely, no horizontal exchange was claimed for Sample A3B1 ("Individual 56" [C]),
386 yet it was another clear outlier in Figure 4. We were not provided with mtCO1 or EPIC25
387 chromatograms for Sample A3B1, but the evidence from 28S suggests that DNA from a second
388 animal was present. Perhaps no interspecific recombination was claimed because the same animal's
389 sequence happened to be in the majority at all loci. The true incidence of cross-contamination may
390 therefore be higher than the six samples where incongruence was noted.

391

392 For Sample B14, we found evidence of an additional EPIC25 haplotype consistent with Species E,
393 even though two EPIC25 haplotypes from Species C had already been reported by Debortoli et al.
394 The match was better than the null expectation by a significant margin ($\chi^2=11.18$, d.f. = 2, $P =$
395 0.00374). The presence of a third EPIC25 haplotype in a single sample is suggestive regardless of its
396 identity, since no single animal in the study of Debortoli et al. had more than two copies of this
397 marker. Only one chromatogram was provided (for the primer EPIC25F), and without the guidance
398 of bidirectional reads for this indel-rich intronic marker, we did not attempt to align other species.

399

400 For Sample B3B1, the only EPIC25 haplotype reported by Debortoli et al. belonged to Species E.
401 However, we found evidence of at least one and possibly two additional EPIC25 haplotypes uniquely
402 matching Species C (Table 1). The fit was very significantly better than the null expectation
403 ($\chi^2=108.44$, d.f. = 2, $P < 2.2 \times 10^{-16}$). Indeed, no other species could be aligned to the secondary
404 peaks, given the indel issues discussed above. The model of "interspecific recombination" and "gene
405 conversion" presented by Debortoli et al. (2016) has difficulty accommodating two different non-

406 native sequences at one locus, in addition to the other more serious obstacles we discuss elsewhere.
407 The 'native' EPIC25 sequence we would predict for Species A was not recovered; we suggest it was
408 dropped during WGA or PCR. At the noisy mtCO1 locus, Species C also showed the strongest
409 evidence of a fit to the minority peaks (Figure S7, $\chi^2=12.9$, d.f. = 2, P = 0.00158), though the fit to
410 Species E also differed significantly from the null expectation ($\chi^2=7.35$, d.f. = 2, P = 0.0254). This
411 evidence points to Species C as one of the contaminants. Our interpretation is that Sample B3B1
412 contained animals or loose DNA belonging to Species A, C and E.

413

414 **5.5 Sample D14**

415

416 Debortoli et al. (2016) interpreted Sample D14 as "Individual 5", and inferred that a Species A
417 EPIC25 sequence had been replaced by Hap10 from Species C. If the incongruent sequence instead
418 reflects amplification from another animal or contaminating DNA from Species C, a native Species A
419 haplotype is expected among the amplicons. Table S3 of Debortoli et al. (2016) seems to predict
420 either Hap1 [A] or Hap4 [A]. In the chromatograms, Hap10 [C] is the majority sequence, but in both
421 directions there is a second haplotype with peaks of almost equal height running several base pairs
422 out of phase, as expected if indels are present. It corresponds exactly to Hap4 [A], with a specific
423 number of GAA tandem repeats to distinguish it from Hap1 [A]. Additional File 4 shows these
424 chromatograms aligned, pointing out peaks matching the second sequence, and highlighting sites
425 where it differs from the Hap 10 [C] interpretation. It was not necessary to attempt to align all the
426 other *Adineta* species to these chromatograms and compare peak heights, as EPIC25 is so variable
427 that no other species would match. Almost all base calls for Hap4 [A] use either first- or second-
428 ranked peaks, and no fourth-ranked peaks are required at all. The probability this could happen by
429 chance is negligible ($\chi^2=75.97$, d.f. = 2, P < 2.2×10^{-16}). The most parsimonious interpretation is that
430 Individual 5 belonged to Species A, and had concordant haplotypes at all loci in the expected
431 combinations. Sample D14 was contaminated with some DNA belonging to Species C, with an
432 EPIC25 haplotype that was amplified by WGA and PCR along with the native haplotype.

433

434 As discussed in the text, Debortoli and colleagues supplied two separate bidirectional pairs of EPIC25
435 chromatograms for Sample D14. Each pair represented an independent PCR amplification from the
436 same DNA sample following WGA (N. Debortoli, pers. comm.). In one chromatogram pair, discussed
437 above, the expected Species A sequence was unambiguous. Importantly, however, this native
438 sequence was absent from the second pair of chromatograms, even as minor secondary peaks
439 (Additional File 4). Even on close scrutiny, only the incongruent sequence from Species C was visible.

440 Clearly, the DNA in the template tube had not changed from one PCR to the next; therefore, the
441 inconsistency arose from complete loss of a haplotype during the dynamics of multi-template PCR.

442

443 **6.0 Genetic identity and microhomology analyses**

444

445 **6.1 Pairwise marker alignments to determine homology between species**

446

447 To determine pairwise homology between sequences involved in “interspecific recombination”, we
448 aligned the putative donor and recipient haplotypes in each case as described above using the
449 MAFFT v. 7.017 algorithm (Kato et al. 2009), implemented via the Geneious plugin (v. 1.3.3) with
450 default settings. We then recorded the pairwise identity for each alignment and the GC content of
451 each sequence, as reported in the Geneious "Statistics" interface.

452

453 **6.2 Validation of pairwise homology calculations for wider genomic regions**

454

455 The genetic distances in Table 2 are estimated for short (<1kb) markers that Debortoli et al. (2016)
456 selected for easy amplification. However, horizontal transfer events are claimed to extend several
457 kilobases beyond the markers they encompass (Figure 5 of Debortoli et al. 2016). We considered
458 the possibility that genomic regions beyond the focal markers might show substantially greater
459 sequence homology between species, thereby decreasing the mechanistic implausibility of HGT. For
460 example, the EPIC25 marker (ca. 400bp) spans the first intron of a gene approximately 4.3kb long,
461 encoding a product with similarity to the vertebrate metastasis suppressor protein 1 (MTSS1). In the
462 *A. vaga* reference genome (Flot et al. 2013), the next-closest gene is approximately 2kb from the
463 marker in a 5' direction, and encodes a product with similarity to vertebrate trifunctional enzyme
464 subunit beta (HADBH). Because introns are often highly variable, pairwise identity at the EPIC25
465 marker might underestimate the homology between two species for the shared genes in this region.

466

467 We tested this hypothesis for the "interspecific recombination" event inferred from Individual 58
468 (Sample B22), in which EPIC25 Hap10 [C] was putatively replaced by Hap37 [E]. At the marker itself,
469 these haplotypes only shared 68.4% genetic identity. We wanted to determine whether the value
470 might be higher if we considered the whole region. While investigating putative intraspecific
471 exchange, Debortoli et al. (2016) sequenced a longer (10.8kb) region surrounding EPIC25 Hap10 for
472 two other individuals in Species C (42 and 51). The region containing the genes *MTSS1* and *HADBH*
473 was syntenic with the *A. vaga* reference genome. To determine the homology between Species C

474 and E, we would ideally align this extended region with its counterpart in Species E, but no
475 sequenced genome for Species E is available. However, the reference genome clone of *A. vaga*
476 ("AD008") happens to be very closely related to Species E (Figure 3). In fact, the percentage
477 homology to Hap10 [C] at the EPIC25 marker is identical (68.4%) for Hap37 [E] and AD008. We
478 compared the equivalent identities at all five available loci, and in each case, the homology to
479 Species C was nearly identical for Species E and the *A. vaga* reference genome (Table S3). This
480 coincidence enabled us to use the *A. vaga* reference genome as a surrogate for Species E, with some
481 confidence that the results would reflect the relationship to Species C.

482

483 We aligned the sequenced EPIC25 region from Individual 42 [C] (GenBank: KU861136.1) against the
484 matching region from the reference genome (Assembly GCA_000513175.1) using MAFFT as
485 implemented in Geneious, with default settings. For clarity, we delineated a focal region from the
486 stop codon of *MTSS1* to the stop codon of *HADBH* (8949bp, approximately centred on EPIC25). This
487 included exons and introns from both complete genes, and the intergenic region. We then
488 measured the pairwise identity between the species for variety of subregions (Table S4).

489

490 The homology between these species for the whole region is 62.3%, which is less than the estimate
491 based on the EPIC25 marker. The intergenic region is very divergent (52.4%), but even if we only
492 compare genes, the values are either lower than the estimate from the EPIC25 marker (for *HADBH*),
493 or identical to it (for *MTSS1*). Thus, we can reject the hypothesis that the marker-based identities in
494 Table 2 underestimate the homology between species for broader genomic regions. The distances
495 involved would remain incompatible with interspecific recombination even if we only looked at
496 discontinuous exons, whose identity was 75.1% for *MTSS1*. This is nearly the same as the mean
497 identity between independently evolving ohnologs in the reference genome (74.8%, Flot et al. 2013).

498

499 **6.3 Methods for microhomology analysis**

500

501 Mechanisms of "interspecific recombination" based on overall homology seemed to be excluded for
502 the sequence pairs we considered, which have equal or lower identities than independently evolving
503 ohnologs within the same genomes (Table 2, Table S4). However, we also considered alternative
504 mechanisms with less stringent identity requirements than HR (N. Debortoli, J.-F. Flot, K. Van
505 Doninck, pers. comm). One example is homology-facilitated illegitimate recombination (HFID), in
506 which "single regions of high nucleotide-sequence similarity (~200 bp in length)...initiate
507 recombination events that lead to the additive integration of >1000-bp-long heterologous DNA

508 fragments" (Thomas & Nielsen 2005). Another is microhomology-mediated end joining (MMEJ),
509 whose "foremost distinguishing property...is the use of 5–25 bp microhomologous sequences during
510 the alignment of broken ends before joining" (McVey & Lee 2008). If interspecifically transferred
511 sequences share longer or more frequent mismatch-free blocks than genomic ohnologs (Vulić et al.
512 1997), then HFID or MMEJ might explain how they could be exchanged frequently while ohnologs
513 with higher global homology evolve independently.

514

515 We estimated the length and frequency of microhomologous blocks for genes surrounding the
516 putative transfer inferred from Sample B22, between EPIC25 Hap10 [C] and EPIC25 Hap37 [E]. As
517 above, we used the genome reference clone for *A. vaga* (AD008) as a surrogate for Species E (Table
518 S3). At every scale from 1-40bp, we compared interspecific microhomology for *MTSS1-A* and *HADBH*
519 with intragenomic microhomology for 7650 ohnologous pairs of genes in the *A. vaga* reference
520 genome. As an important point of comparison, we highlighted the microhomology between *MTSS1-*
521 *A* and its own genomic ohnolog (*MTSS1-B*), which contains the EPIC63 marker. Debortoli et al.
522 (2016) implicitly assume there is no exchange between these highly divergent genes, which were
523 treated as "independent nuclear markers" and sequenced with "ohnologue-specific" primers.

524

525 Gene models for *A. vaga* were constructed using BRAKER (Hoff et al. 2015), with RNASeq as evidence
526 (SRA accession: ERR260376; Flot et al. 2013). Collinear regions were identified using MCScanX (Wang
527 et al. 2012), setting the maximum number of allowed gaps between collinear genes to 10. Between
528 all pairs of collinear genes, synonymous (K_s) and nonsynonymous (K_A) divergences were calculated
529 using the method of Nei & Gojobori (1986), implemented in BioPerl (Stajich et al. 2002). Ohnologs
530 were defined as pairs of genes within collinear regions with $K_s \geq 0.5$ ($n = 7,650$). Ohnologous regions
531 (comprising exons plus introns) were extracted and aligned using MAFFT (Katoh & Standley 2013)
532 with default settings. Introns were included because intronic markers were claimed to show
533 interspecific recombination, and any inter-ohnolog recombination facilitated by microhomology
534 would involve unspliced genomic DNA. Microhomology across all 7,650 alignments was calculated
535 with a custom Perl script, using a sliding window approach along each alignment (sliding one base
536 each iteration), from a window size of one to 40 bp, and counting any window of exact identity as a
537 match. The number of identical blocks was scaled relative to the length of each alignment to account
538 for variation in gene length, and multiplied by 1,000 to give a per-kb estimate. All scripts are
539 available at <https://github.com/reubwn/microhomology>. The same method was used to measure
540 microhomology between Species C and *A. vaga* for the alignments of *MTSS1-A* and *HADBH* discussed

541 above. Finally, we highlighted the specific microhomology curve in *A. vaga* corresponding to the
542 pairing between *MTSS1-A* and its ohnolog, *MTSS1-B*.

543

544 Gene copies involved in putative interspecific recombination did not share significantly more or
545 longer blocks of microhomology than independently evolving ohnologs in the same genomes, at any
546 scale from one to 40bp (Figure S9). At most scales they even shared less microhomology with the
547 "donor species" than with their own ohnologs. Microhomology-based mechanisms such as MMEJ
548 and HFIR could not facilitate distant interspecific recombination and yet fail to permit exchange
549 between ohnologs with even higher microhomology, especially as conspecific DNA fragments seem
550 likely to be more abundant and available than heterospecific ones.

551

552 Other mechanisms of homology recognition seem even less applicable. For instance, pairing of
553 chromosomes early in meiosis appears to be independent of recombination in some cases (Da Ines
554 et al. 2014), but this involves chromosome-scale features such as centromeres and telomeres, which
555 are not shared by loose DNA fragments. Pairing must still be stabilised by recombination, via
556 sequence-dependent pathways. Another recognition mechanism involves homologous trinucleotide
557 repeats interspersed at a specific periodicity within otherwise divergent sequences (Gladyshev &
558 Kleckner 2016), but there is no evidence for this distinctive architecture in the putatively exchanged
559 sequences we examined, and that pathway is not linked to recombination. It seems improbable
560 *prima facie* that any mechanism could enable ready exchange of DNA across species boundaries,
561 while simultaneously precluding exchange between less divergent ohnologs within the same
562 genomes. We suggest that any argument to the contrary ought to bear the burden of proof.

563

564

565

566

567

568

569

570

571

572

573

574

575 **Supplementary References**

576

577

578 1. Agresti, A. (2007). *An introduction to categorical data analysis*. 2nd edn. John Wiley & Sons, Inc.,
579 Hoboken, New Jersey

580

581 2. Barron, G. (2004). Fungal parasites and predators of rotifers, nematodes, and other invertebrates.
582 In: *Biodiversity of fungi: inventory and monitoring methods* (eds. Mueller, G.M., Bills, G.F. & Foster,
583 M.S.). Elsevier Academic Press, San Diego, pp. 435–450

584

585 3. Davis, H. (1873). A new *Callidina*: with the result of experiments on the desiccation of rotifers.
586 *Mon. Microsc. J.*, 9, 201–209

587

588 4. Debortoli, N., Li, X., Eyres, I., Fontaneto, D., Hespeels, B., Tang, C.Q., *et al.* (2016). Genetic
589 exchange among bdelloid rotifers is more likely due to horizontal gene transfer than to meiotic sex.
590 *Curr. Biol.*, 26, 723–732

591

592 5. Ewing, B. & Green, P. (1998). Base-calling of automated sequencer traces using phred. II. Error
593 probabilities. *Genome Res.*, 8, 186–194

594

595 6. Flot, J., Hespeels, B., Li, X., Noel, B., Arkhipova, I., Danchin, E.G.J., *et al.* (2013). Genomic evidence
596 for ameiotic evolution in the bdelloid rotifer *Adineta vaga*. *Nature*, 500, 453–457

597

598 7. Folmer, O., Black, M., Hoeh, W., Lutz, R. & Vrijenhoek, R. (1994). DNA primers for amplification of
599 mitochondrial cytochrome *c* oxidase subunit I from diverse metazoan invertebrates. *Mol. Mar. Biol.*
600 *Biotechnol.*, 3, 294–299

601

602 8. Gladyshev, E. & Kleckner, N. (2016). Recombination-independent recognition of DNA homology
603 for repeat-induced point mutation (RIP) is modulated by the underlying nucleotide sequence. *PLoS*
604 *Genet.*, 12, e1006015

605

- 606 9. Han, T., Chang, C.-W., Kwekel, J.C., Chen, Y., Ge, Y., Martinez-Murillo, F., *et al.* (2012).
607 Characterization of whole genome amplified (WGA) DNA for use in genotyping assay development.
608 *BMC Genomics*, 13, 217
- 609
- 610 10. Hoff, K.J., Lange, S., Lomsadze, A., Borodovsky, M. & Stanke, M. (2015). BRAKER1: Unsupervised
611 RNA-Seq-based genome annotation with GeneMark-ET and AUGUSTUS. *Bioinformatics*, 32, 767–769
- 612
- 613 11. Da Ines, O., Gallego, M.E. & White, C.I. (2014). Recombination-independent mechanisms and
614 pairing of homologous chromosomes during meiosis in plants. *Mol. Plant*, 7, 492–501
- 615
- 616 12. Katoh, K., Asimenos, G. & Toh, H. (2009). Multiple alignment of DNA sequences with MAFFT.
617 *Methods Mol. Biol.*, 537, 39–64
- 618
- 619 13. Katoh, K. & Standley, D.M. (2013). MAFFT multiple sequence alignment software version 7:
620 Improvements in performance and usability. *Mol. Biol. Evol.*, 30, 772–780
- 621
- 622 14. Kearse, M., Moir, R., Wilson, A., Stones-Havas, S., Cheung, M., Sturrock, S., *et al.* (2012).
623 Geneious Basic: An integrated and extendable desktop software platform for the organization and
624 analysis of sequence data. *Bioinformatics*, 28, 1647–1649
- 625
- 626 15. Larosa, V. & Remacle, C. (2013). Transformation of the mitochondrial genome. *Int. J. Dev. Biol.*,
627 57, 659–665
- 628
- 629 16. Mark Welch, J.L. & Meselson, M. (1998). Karyotypes of bdelloid rotifers from three families.
630 *Hydrobiologia*, 387, 403–407
- 631
- 632 17. McVey, M. & Lee, S.E. (2008). MMEJ repair of double-strand breaks (director’s cut): deleted
633 sequences and alternative endings. *Trends Genet.*, 24, 529–538
- 634
- 635 18. Mullis, K.B., Ferre, F. & Gibbs, R.A. (1994). *The polymerase chain reaction*. Birkhäuser, Boston

636
637
638
639
640
641
642
643
644
645
646
647
648
649
650
651
652
653
654
655
656
657
658
659
660
661
662
663
664
665

19. Nei, M. & Gojobori, T. (1986). Simple methods for estimating the numbers of synonymous and nonsynonymous nucleotide substitutions. *Mol. Biol. Evol.*, 3, 418–426

20. Polz, M.F. & Cavanaugh, C.M. (1998). Bias in template-to product ratios in multitemplate PCR. *Appl. Environ. Microbiol.*, 64, 3724–3730

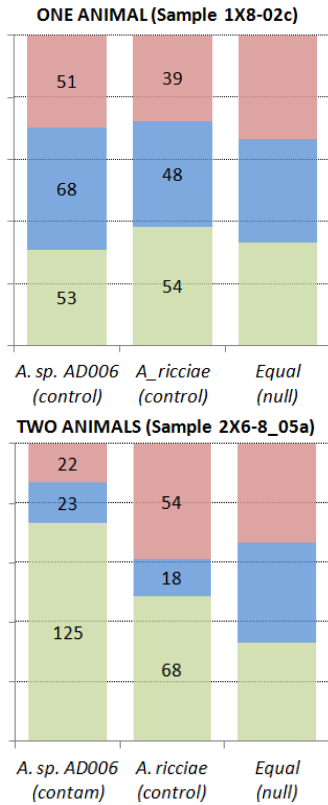
21. Stajich, J.E., Block, D., Boulez, K., Brenner, S.E., Chervitz, S.A., Dagdigian, C., *et al.* (2002). The Bioperl toolkit: Perl modules for the life sciences. *Genome Res.*, 12, 1611–1618

22. Thomas, C.M. & Nielsen, K.M. (2005). Mechanisms of, and barriers to, horizontal gene transfer between bacteria. *Nat. Rev. Microbiol.*, 3, 711–721

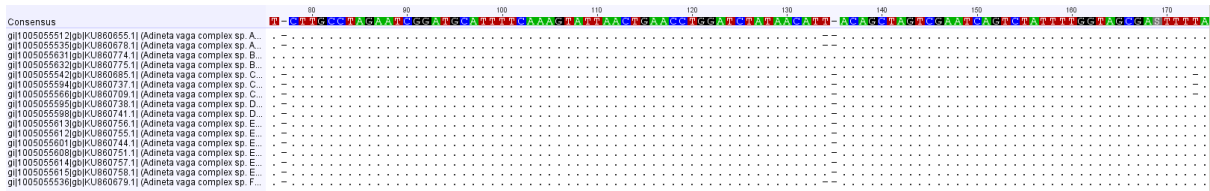
23. Vulić, M., Dionisio, F., Taddei, F. & Radman, M. (1997). Molecular keys to speciation: DNA polymorphism and the control of genetic exchange in enterobacteria. *Proc. Natl. Acad. Sci. U. S. A.*, 94, 9763–7

24. Wang, Y., Tang, H., Debarry, J.D., Tan, X., Li, J., Wang, X., *et al.* (2012). MCScanX: A toolkit for detection and evolutionary analysis of gene synteny and collinearity. *Nucleic Acids Res.*, 40, e49

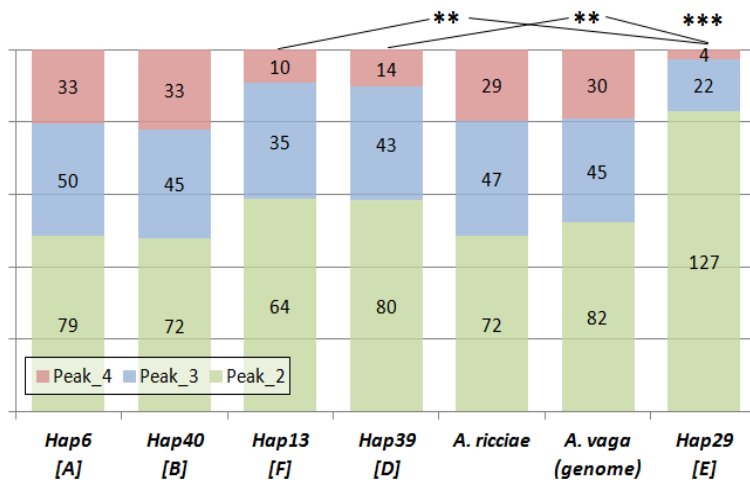
25. Wilson, C.G. & Sherman, P.W. (2010). Anciently asexual bdelloid rotifers escape lethal fungal parasites by drying up and blowing away. *Science*, 327, 574–576



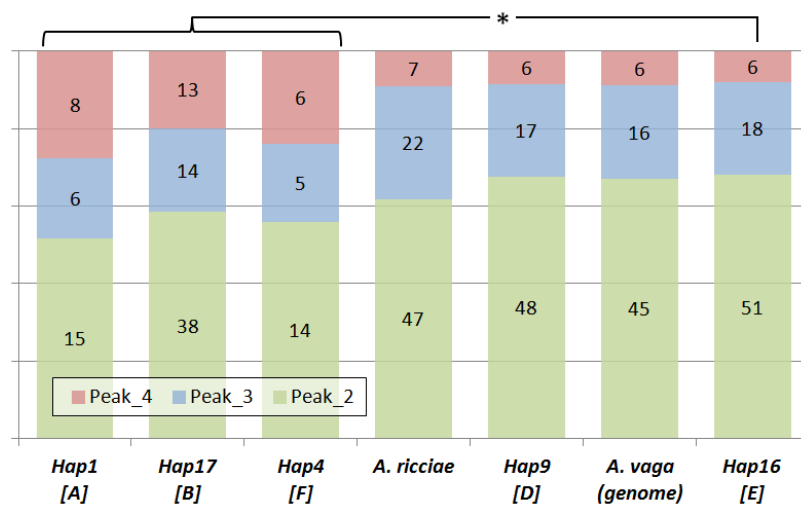
666 **Figure S1.** Minority peak analysis of mtCO1 chromatograms for two samples where *A. vaga* (AD008)
 667 was in the majority. In the first sample, *A. vaga* was the only rotifer present, and the fit of minority
 668 peaks to other haplotypes did not differ significantly from the null expectation. In the second
 669 sample, another rotifer belonging to *Adineta* sp. (AD006) was present, and minority peaks
 670 corresponding to this known contaminant were a significantly better fit than the null expectation
 671 ($\chi^2=123.61$, d.f. = 2, $P < 2.2 \times 10^{-16}$), or a control species, *A. ricciae* ($\chi^2=28.28$, d.f. =2, $P = 7.23 \times 10^{-7}$).
 672
 673



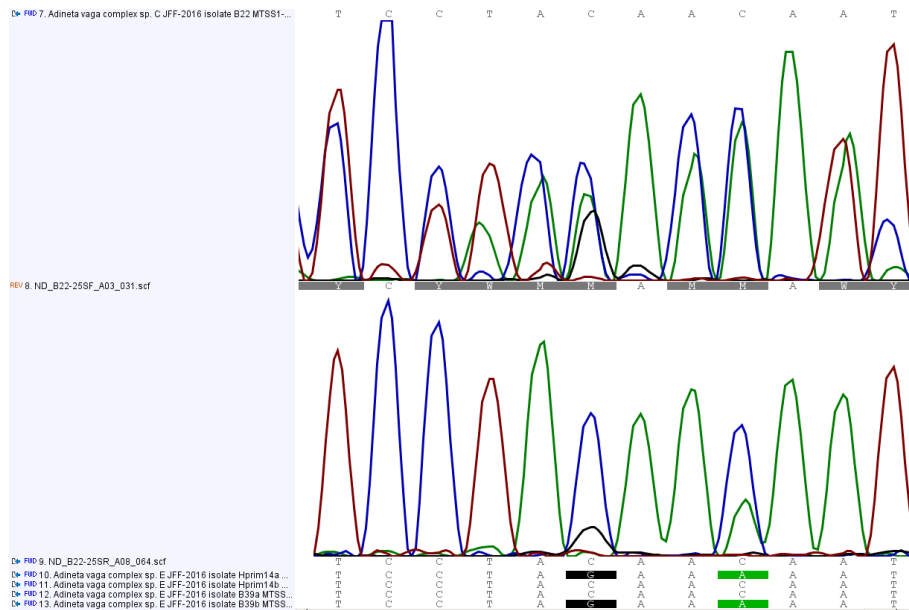
674 **Figure S2.** Insertion-deletion polymorphisms in an alignment of 28S ribosomal DNA sequences for
 675 the six *Adineta* species reported by Debortoli et al. (2016). Dots indicate agreement to the
 676 consensus sequence; dashes indicate gaps. Minority and majority sequences of different lengths are
 677 predicted to run out of phase in chromatograms for part of their length.



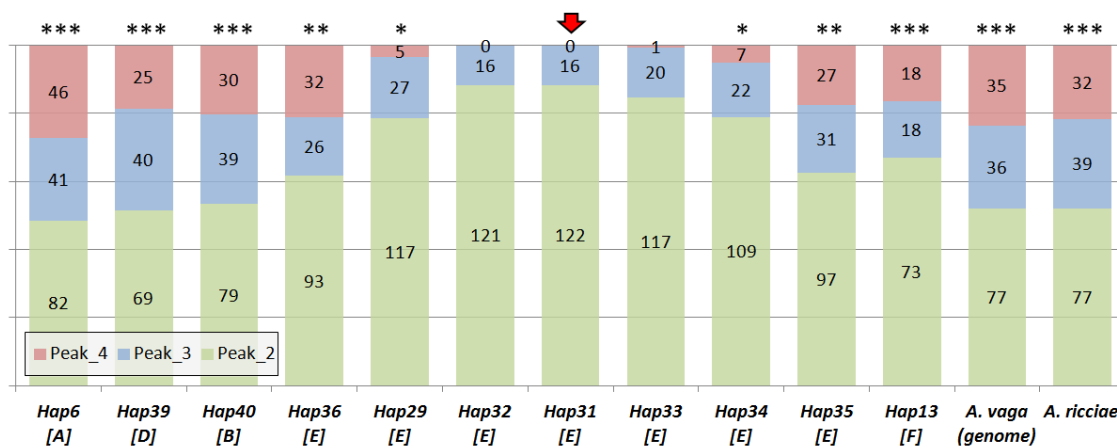
678 **Figure S3.** Summary of minority peaks in mtCO1 chromatograms for Sample B22. The fit of Hap29
 679 [E] is significantly better (***) than the other six species ($\chi^2=69.49$, d.f. = 12, $P = 3.99 \times 10^{-10}$). If
 680 Hap29 [E] is removed, the other distributions are not significantly different from one another
 681 ($\chi^2=15.2$, d.f. = 10, $P = 0.124$). If compared directly, Hap29 [E] is a significantly better fit (**)
 682 either Hap13 [F] ($\chi^2=19.48$, d.f. = 2, $P = 5.9 \times 10^{-5}$) or Hap 39 [D] ($\chi^2=22.2$, d.f. = 2, $P = 1.51 \times 10^{-5}$).
 683



684 **Figure S4.** Summary of minority peaks in 28S chromatograms for Sample B22. Hap 16 [E] is a
 685 significantly better fit to these peaks (*) than Hap1 [A], Hap 17 [B] and Hap4 [E], which were pooled
 686 owing to small cell counts ($\chi^2=6.85$, d.f. = 2, $P = 0.029$). The remaining species are too closely
 687 related to Species E to be distinguished statistically at the highly conserved 28S locus.
 688



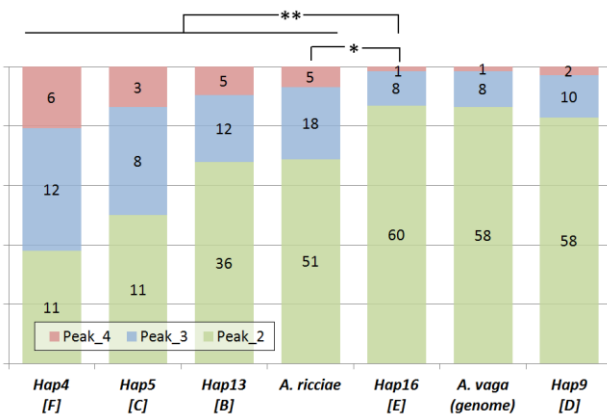
689 **Figure S5.** Shifted and double peaks in EPIC25 chromatograms for Sample B22 indicate indels and
 690 SNPs between two homologous sequences, both belonging to Species E and incongruent with the
 691 Species C background. The two SNPs shown here correspond to polymorphisms seen natively in
 692 "heterozygous" animals from the Species E population (Hprim14a/b and B39a/b). Horizontal import
 693 of standing heterozygosity is not predicted in the model of interspecific recombination presented by
 694 Debortoli et al. (2016), but it is predicted if the sequences arise from cross-contamination.
 695



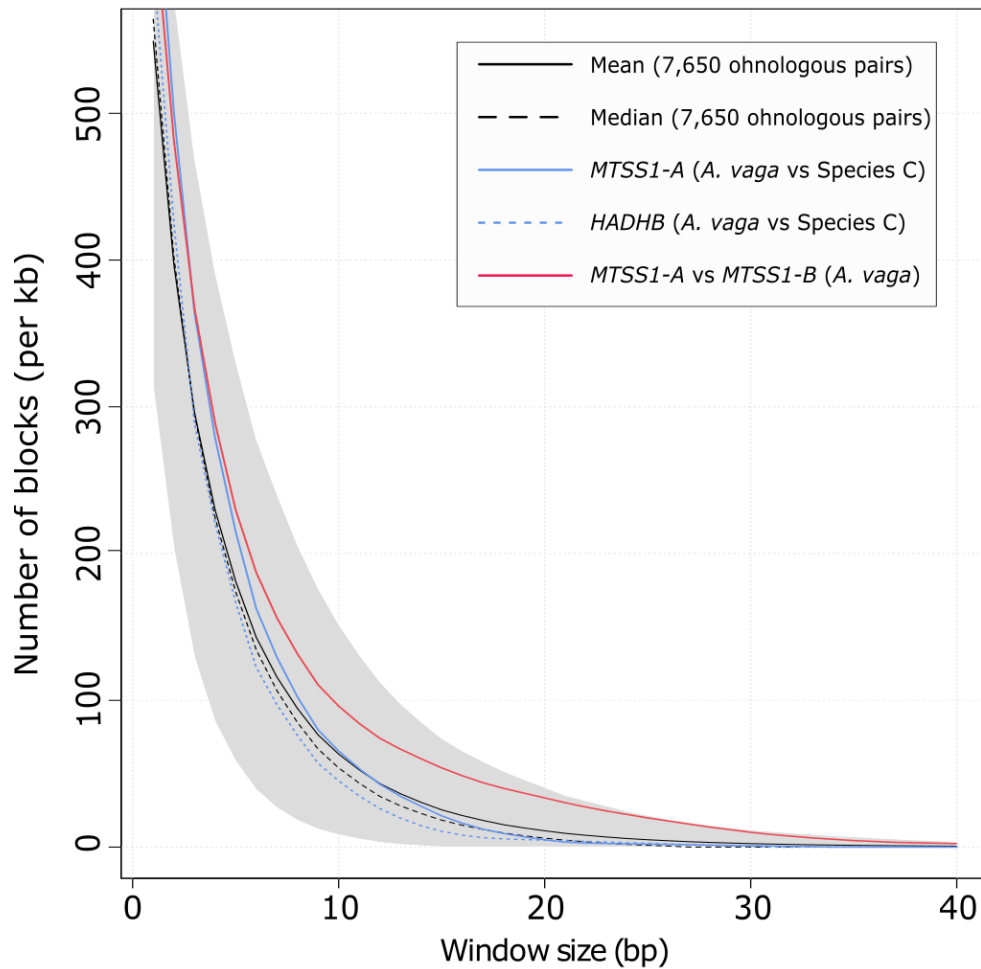
696 **Figure S6.** Minority peaks in mtCO1 chromatograms for Sample B39 (Individual 66) indicate the
 697 predicted 'native' haplotype Hap31 [E] (red arrow), and challenge the hypothesis that mtDNA has
 698 undergone interspecific recombination. Hap31 [E] is a significantly better match to the secondary
 699 peaks than all other haplotypes (*: $\chi^2 = 9.63$, d.f. = 4, $P = 0.047$; **: $\chi^2 = 66.71$, d.f. = 8, $P = 2.21 \times 10^{-11}$;
 700 ***: $\chi^2 = 136$, d.f. = 20, $P < 2.2 \times 10^{-16}$), except Hap32 [E] and Hap33 [E], which are nearly identical and
 701 were not included in contingency table tests.



702 **Figure S7.** Analysis of minority peak distributions indicates additional mtCO1 sequences in
 703 chromatograms for Samples B14 and B3B1. Multiple candidate haplotypes are a significantly better
 704 fit than expected under a null distribution of peak ranks (*** : $P < 0.001$, **: $P < 0.01$; *: $P < 0.05$),
 705 but their distributions do not differ significantly when compared with each other, and we cannot
 706 therefore narrow down a single minority haplotype driving the pattern. Two different
 707 contaminating sequences may be superimposed in each case, alongside the Species A majority
 708 haplotype. Clear evidence for haplotypes from Species A, C and E was found at other loci.
 709



710 **Figure S8.** Minority peaks in 28S chromatograms for Sample B14 reveal a second haplotype that fits
 711 Species E significantly better than Species B, C, F or *A. ricciae* (**: $\chi^2 = 28.77$, d.f. = 8, $P = 3.0 \times 10^{-4}$; * :
 712 $\chi^2 = 7.1$, d.f. = 2, $P = 0.029$). Hap9 [D] and *A. vaga* (genome) are nearly identical to Hap16 [E] and
 713 cannot be distinguished statistically.



715 **Figure S9.** Two genes linked to an "interspecific horizontal genetic transfer" event did not share
 716 significantly more or longer microhomologous blocks than 7650 pairs of independently evolving
 717 ohnologous genes in the *A. vaga* reference genome. Regardless of scale (1-40bp), the degree of
 718 microhomology between "transferred" sequences (blue lines) falls within the 5% and 95% quantiles
 719 for genomic ohnologs (grey shading). The dashed blue line represents the gene *MTSS1-A*, containing
 720 the EPIC25 marker; the solid blue line shows the next-closest gene (*HADHB*). For sliding windows
 721 above 3bp, the "horizontally transferred" *MTSS1-A* sequences share less microhomology with each
 722 other than with their own independently evolving ohnolog (*MTSS1-B*) in the same genome (red line).

723

724

725

726

727

728
729
730

Group name	1X6	1X8	2X6-8
Animals	One: AD006	One: AD008	Two: AD006 and AD008
Biological replicates	3	2 (1 lost)	6
Technical replicates	1 triplicate, 2 single	1 triplicate, 1 single	1 triplicate, 2 duplicate, 3 single

731
732
733
734
735

Table S1. Design and replication of an experiment to determine the effect of multiple rotifers in a single DNA extraction tube. AD006: *A. sp.* ‘AD006’; AD008: *A. vaga* (reference genome clone).

Sample code	Majority haplotype	Minority haplotype	Number of chromatogram files	Total bases called	Minority base calls	% sites with majority calls
01	<i>A. sp.</i> (AD006)	<i>A. vaga</i> (AD008)	2 (singleton)	1210	25	97.94
02	<i>A. vaga</i> (AD008)	<i>A. sp.</i> (AD006)	2 (singleton)	1210	5	99.59
03	<i>A. sp.</i> (AD006)	<i>A. vaga</i> (AD008)	4 (duplicated)	2420	8	99.66
04	<i>A. vaga</i> (AD008)	<i>A. sp.</i> (AD006)	2 (singleton)	1210	6	99.5
05	<i>A. vaga</i> (AD008)	<i>A. sp.</i> (AD006)	4 (duplicated)	2420	16	99.33
06	<i>A. sp.</i> (AD006)	<i>A. vaga</i> (AD008)	6 (triplicated)	3630	13	99.64

736
737
738
739
740
741

Table S2. Summary of base calls from ABI Sanger sequencing of mtCO1, corresponding to majority and minority haplotypes for biological and technical replicates of experimentally contaminated samples (Group 2X6-8). Chromatograms are always in bidirectional pairs.

Marker	Species C	Species E	C vs. E (%)	C vs. ref (%)
mtCO1	Hap10 (KU860596)	Hap29 (KU860588)	87.8	87.8
28S	Hap5 (KU860706)	Hap16 (KU860768)	97.6	97.7
EPIC25	Hap10 (KU860907)	Hap37 (KU860804)	68.4	68.4
EPIC63	Hap4 (KU860934)	Hap34 (KU860927)	67.4	67.6
Nu1054	Hap16 (KU861061)	Hap21 (KU861052)	70.1	70.2

742
743
744
745
746
747

Table S3. At five independent mitochondrial and nuclear marker loci, the percentage identity between Species C and Species E is almost exactly reproduced by comparing Species C to the reference genome of *A. vaga*. The reference genome therefore is an appropriate surrogate for Species E when estimating homology parameters for a hypothetical transfer from Species C.

Comparison	Aligned length (bp)	Identity (%)
EPIC25 marker only	395	68.4
Two-gene region	8949	62.3
<i>MTSS1</i> whole gene	4419	68.4
<i>MTSS1</i> exons	2301	75.1
<i>MTSS1</i> introns	2118	61.1
Intergenic region	2203	52.4
<i>HADBH</i> whole gene	2327	60.1
<i>HADBH</i> exons	1605	67.0
<i>HADBH</i> introns	722	44.7

748

749 **Table S4.** Pairwise identity between Species C and the *A. vaga* reference genome for the region
750 surrounding the EPIC25 marker. Regardless of the scope or scale of the comparison, the distances
751 are not compatible with the "interspecific recombination" claimed between Species C and Species E.
752 The identity estimate from the short EPIC25 marker accurately reflects (or even overestimates)
753 homology more broadly.